The New Challenges of Brain PET Imaging Technology

Habib Zaidi* and Marie-Louise Montandon

Geneva University Hospital, Division of Nuclear Medicine, CH-1211 Geneva, Switzerland

Abstract: During the last two decades, functional brain imaging using positron emission tomography (PET) has advanced elegantly, and steadily gained importance in the clinical and research arenas. Significant progress has been made by different scanner manufacturers and research groups in the design of dedicated high-resolution three-dimensional (3-D) PET units; however, emerging clinical and research applications of functional brain imaging promise even greater levels of accuracy and precision and therefore, impose more constraints with respect to the intrinsic performance of the PET tomograph. Continuous efforts to integrate recent research findings for the design of different geometries and various detector/readout technologies of PET scanners have become the goal of both the academic community and nuclear medicine industry. As PET has become integrated into clinical practice, several design trends have developed; with systems now available with a spectrum of features, from those designed for "low cost" clinical applications to others designed specifically for very high-resolution research applications. There is also a continual upward revision and refinement in both hardware and software components for all of these systems.

Software- and hardware-based correlation between anatomical (x-ray CT, MRI) and physiological (PET) information is a promising research field and now offers unique capabilities for the medical imaging community and biomedical researchers. One of the main advantages of dual-modality PET/CT imaging is that PET data are intrinsically aligned to anatomical information from the x-ray CT without the use of external markers or internal landmarks, thus providing a reliable estimate of the attenuation map to be used for attenuation and scatter correction purposes. On the other hand, combining PET with MRI technology is scientifically more challenging owing to the strong magnetic fields. Nevertheless, significant progress has been made resulting in the design of a prototype small animal PET scanner coupled to three multi-channel photomultipliers via optical fibers, so that the PET detector can be operated within a conventional MR system. Thus, many different design paths have been and continue to be pursued in both academic and corporate settings, that offer different trade-offs in terms of their performance. It still is uncertain which designs will be incorporated into future clinical and research systems, but it is certain that technological advances will continue and will enable new quantitative capabilities in brain PET imaging. This paper briefly summarizes state of the art developments in dedicated brain PET instrumentation. Future prospects will also be discussed.

Keywords: Positron emission tomography, functional brain imaging, instrumentation, detectors, dual-modality imaging.

1. INTRODUCTION

The historical development of positron emission tomography (PET) is marked by numerous significant technological accomplishments driven by an unprecedented collaboration between multi-disciplinary groups of investigators with backgrounds in medical sciences, physics, chemistry, mathematics, bioengineering, and computer science [1]. The first medical applications of positron radiation focused on the brain; thanks to the pioneering work of Brownell, Sweet and colleagues at Massachusetts General Hospital who devised the first apparatus based on coincidence detection to localize brain tumors [2-4]. Likewise, most of the first human PET prototypes were developed specifically for functional brain imaging including the PET III developed by Phelps and colleagues [5, 6]; PC-II [7], Positome II [8], as well as PETTV [9] and PETTVI [10] tomographs built in the late 70s using sodium iodide (NaI(Tl)) and Cesium Fluoride (CsF) crystals, respectively. Many other designs have also been developed in the early 80s including the Positologica [11], HEADTOME [12], Neuro-PET [13], Scanditronix PC384-7b [14] and PC2048-15B [15], NeuroECAT [16, 17], the Hamamatsu SHR 1200/2400 tomographs [18] and the CTI/Siemens ECAT 953B [19], considered as state of the art technology in the early 1990s.

Modern commercially available dedicated full-ring PET tomographs are considered to provide state of the art performance [20-26]. The improved performance of dedicated systems compared to camera-based dual or triple-headed systems is due to higher overall system efficiency and count rate capability, which provides the statistical realization of the physical detector resolution and not a higher intrinsic physical detector resolution [27]. Figure **1** illustrates historical developments highlighting the improvement in image quality and spatial resolution of clinical brain PET images resulting from the improvement of both the intrinsic performance of PET scanners and image correction and reconstruction algorithms. Both the academic community and the nuclear medicine industry maintain a continuous learning cycle and assessment of products quality to advance the technology and the operational capabilities of PET tomographs. As PET has become integrated into clinical practice, several design trends have developed, with systems now available with a spectrum of features, from those

*Address correspondence to this author at Geneva University Hospital, Division of Nuclear Medicine, CH-1211 Geneva, Switzerland; Tel: +41 22 372 7258; Fax: +41 22 372 7169; E-mail: habib.zaidi@hcuge.ch

1573-4056/06 $50.00+.00

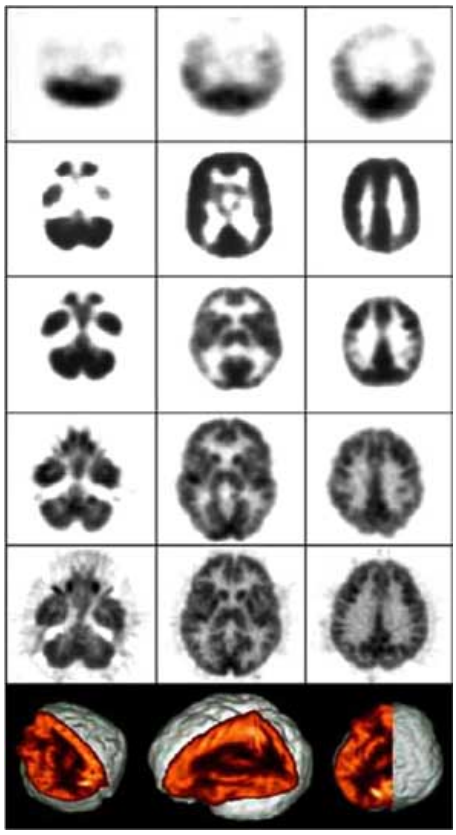

Fig. (1). Illustration of the significant improvement in clinical ^{18}F-FDG brain PET image quality and spatial resolution resulting from the improvement in scanner performance for each generation during the last three decades (Reproduced from CTI Molecular Imaging web site).

designed for clinical whole-body applications to others designed specifically for very high-resolution brain research applications. There is also a continual upward revision and refinement in both hardware and software components for all of these systems. In parallel to these developments and ongoing research in software-based image co-registration and fusion [28], hardware dual-modality imaging, an approach where two different imaging techniques are integrated in a single unit that allows imaging with both approaches during a single experimental procedure (e.g PET/CT and PET/MRI) are under development by different research groups and scanner manufacturers. Combined units offer unique capabilities beyond those available from systems that perform radionuclide imaging alone [29]. The visual quality and quantitative accuracy of the PET data can be improved by using fusion with the correlated x-ray CT with the possibility to use them to correct the radionuclide data for perturbations arising from photon attenuation and Compton scatter. There are, however, several important challenges that must be overcome in implementing and operating a combined PET/MRI imaging system, which are discussed in section 4 [30].

Theoretically, an ideal PET tomograph should have high sensitivity and counting rate capability in addition to low dead-time losses, and provide a uniform spatial and energy resolution over the whole sensitive volume allowing to reach the highest signal-to-noise ratio (SNR) for the lowest possible injected activity. Perfect correction for variable crystal detection efficiency and geometrical factors, randoms, scatter, attenuation, partial volume and other background effects is also highly desired to allow accurate measurement of quantitative indices *in vivo*.

2. PROGRESS IN DETECTOR TECHNOLOGY FOR PET

2.1. Scintillation Crystals

The critical component of PET tomographs is the scintillation detector [31]. The scintillation process involves

Table 1. Characteristics of Scintillation Crystals Used or Developed Specifically for the Design of Current Generation PET Imaging Systems

Scintillator	BGO	LSO	GSO	LuAP	$LaBr_3$	LYSO
Formula	$Bi_4Ge_3O_{12}$	Lu_2SiO_5:Ce	Gd_2SiO_5:Ce	$LuAlO_3$:Ce	$LaBr_3$:Ce	$LuYSiO_5$:Ce
Density (g/cc)	7.13	7.4	6.71	8.34	5.3	7.1
Light yield (photons/keV)	9	25	8	10	61	32
Effective Z	75	66	60	65	46.9	64
Principal decay time (ns)	300	42	60	18	35	48
Peak wavelength (nm)	480	420	440	365	358	420
Index of refraction	2.15	1.82	1.95	1.95	1.88	1.8
Photofraction (%)*	41.5	32.5	25	30.6	15	34.4
Attenuation length (cm)*	1.04	1.15	1.42	1.05	2.13	1.12
Energy resolution (%)*	12	9.1	7.9	11.4	3.3	7.1
Hygroscopic	No	No	No	No	Yes	No

*@ 511 keV

the conversion of photons energy into visible light via interaction with a scintillating material. Increased light yield, faster rise and decay times, greater stopping power and improved energy resolution, linearity of response with energy, in addition to low cost, availability, mechanical strength, moisture resistance, and machinability are the desired characteristics of scintillation crystals [32]. Table **1** summarizes most of these properties for selected scintillators currently in use or under development for PET applications [33]. Improvements in these characteristics enable detectors to be divided into smaller elements, thus increasing resolution and minimizing dead-time losses.

The choice of the scintillator is a fundamental element of a PET design. The selection is generally made after careful consideration of the physical characteristics mentioned above. Bismuth germanate (BGO) has a very high physical density and effective atomic number, and is not hygroscopic. These properties rendered it the preferred scintillator for commercial PET units in the 1990s. Its major disadvantages are, however, the low light yield and only a moderately fast decay time that limits coincidence timing and count rate performance.

New detection technologies that are emerging include the use of new cerium doped crystals as alternatives to conventional BGO crystals, and the use of layered crystals and other schemes for depth-of-interaction (DOI) determination, a renewed interest in old technologies such as time-of-flight (TOF) PET [34], taking advantage of excellent timing resolution of new scintillators [35], along with many other designs. It appears that cerium doped lutetium orthosilicate (LSO:Ce) produced by CTI Molecular Imaging (Knoxville, TN), lutetium yttrium orthosilicate (LYSO:Ce) produced by Photonic Materials Ltd. (Bellshill, UK) and cerium doped lanthanum bromide ($LaBr_3$:Ce), under development by Saint Gobain (France), are the most promising candidates [36]. They combine high density and high atomic number necessary for an efficient photoelectric conversion of the annihilation photons, with a short decay time of the scintillation light, which is a key requirement for high counting rates. Phoswich detectors received considerable attention for the design of high-resolution scanners dedicated for brain, female breast and small animal imaging. This may be implemented with solid-state photodiode readouts, which also allows electronically collimated coincidence counting. Such a design has been implemented on the ECAT high-resolution research tomograph (HRRT) with LSO crystals and photomultiplier tubes (PMT's)-based readout [37]. Fig. **2** illustrates the principle of the conventional detector block [38] and the phoswich approach [39], where two detectors are assembled in a sandwich-like design; the difference in decay time of the light is used to estimate depth in the crystal where the interaction occurred. The recently proposed axial arrangement of a matrix of long scintillator crystals readout on both extremities by hybrid photon detectors with matched segmentation is also shown [40].

In the conventional detector block concept, each block (e.g. 8x8 crystals) is readout by an arrangement of 4 standard PMT's optically coupled to the block by means of a light guide, which spreads the light from the individual crystals over all 4 PMT's. The centroid corresponds to the true interaction point of the annihilation photon, in case of conversion by photoelectric effect, or to the energy averaged mean position of the interaction in case of occurrence of Compton scattering in the detector. The phoswich technique is able to roughly halve the uncertainty of the DOI, and hence significantly reduces the parallax error, which is inherent to all radial geometries (Figs. **3**-**4**). However, the phoswich approach is still only a compromise between the maximum crystal length, which can be tolerated for parallax error reasons, and the minimum length which is required to achieve high detection efficiency. In addition, the phoswhich approach demands a delicate pulse shape discrimination of the analog signal delivered by the PMT's in order to identify the hit crystal layer. The readout electronics becomes inevitably more complex and possibly limits the data acquisition rate. The axial arrangement of long finely segmented arrays of long high-Z scintillation crystals coupled to highly pixelated photodetectors leads to an essentially parallax free geometry, which allows reconstructing the interaction point of the annihilation photon in true 3-D reconstruction [41].

2.2. Photodetectors

Recent developments in photodetectors for medical applications should enable efficient collection of the light emanating from the scintillation crystals [42]. The design of high resolution imaging devices imposes some additional constraints with respect to the necessity for compact arrays of photodetectors; in turn, this has stimulated the development and use of multichannel position-sensitive photomultiplier tubes (PS-PMT's), Silicon p-i-n photodiodes (PDs) and avalanche photodiodes (APDs). Solid-state photodiodes exhibit many advantages compared to conventional PMT's. They are relatively small, operate at much smaller voltage, and more importantly, exhibit higher quantum efficiencies. Furthermore, photodiodes are insensitive to axial and transversal strong magnetic fields and therefore, have the potential to be operated within MRI systems. By using this technology, the sensitive area of the detector could be read out more efficiently, taking advantage of recent developments of monolithic pixelated photodetectors. Thanks to the progress made in the microelectronic industry, high-purity detector grade silicon now is available commercially and can be used to produce low-noise silicon planar photodiodes, avalanche photodiodes, and silicon drift photodetectors [43]. Commercially available APDs typically are not pixelated and can have a sensitive area of ~20 mm^2. PDs and APDs can also be segmented to form a linear or two-dimensional array of pixels on a single device [44]. Their geometry can be modified to suit specific applications, with the configuration of the scintillator matrix adapted to the available read out pixelation of the photodetector. However, given the current cost of solid-state photodiodes, they need to offer very significant advantages to replace the currently adopted technology.

Although not previously used in medical imaging, hybrid photodetectors (HPDs) represent an interesting technology with potential for high-resolution photon detection [45]. An HPD consists of a phototube with two key components: a

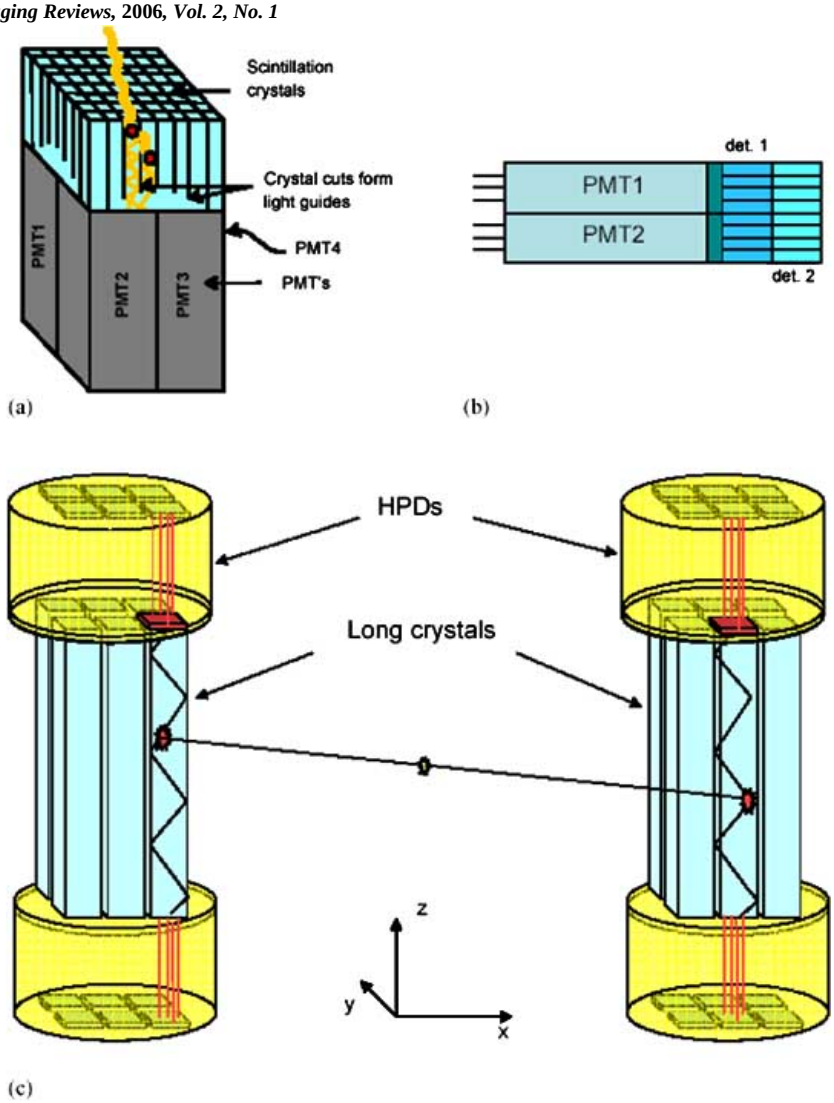

Fig. (2). Sketch of the range of different geometrical arrangements of PET detector modules. (a) Conventional radial arrangement of block detectors consisting of a set of crystals having cuts of different depths acting as light guides and segmenting the block into 64 (8x8) detection elements in this example. The block is optically coupled to four photomultiplier tubes at the back, and the crystal in which photon absorption occurs is identified by comparing the outputs of the four photomultiplier tubes (Anger logic). (b) Detector block consisting of a phoswich (detector 1 and 2) with depth-of-interaction measurement capability. (c) Axial arrangement of a matrix of long scintillator crystals readout by hybrid photon detectors (HPDs) with matched segmentation. In this prototype configuration, two round HPD photodetectors are coupled to the matrix of scintillators.

semi-transparent photocathode (deposited by vacuum evaporation on the entrance window) with high sensitivity for photons in the visible and near UV range, and a silicon (Si) sensor which serves as the anode [46]. The photocathode receives light from a scintillator and converts the incident photons to electrons. These photoelectrons are accelerated by an electrostatic field (10-20 kV between cathode and anode), which is shaped by a set of ring electrodes, onto the segmented Si sensor; the anode thereby creates a signal proportional to the kinetic energy of the incident photoelectrons. In this way, the HPD combines the sensitivity to single photons of a conventional PMT with the spatial and energy resolution of a solid-state sensor. In addition, this design overcomes the intrinsic limitations of a classical PMT with respect to the statistical fluctuations in the number of electrons at the first dynodes. Proximity focused HPDs can be operated in strong magnetic fields, as long as the field direction is aligned with the tube axis. Axial magnetic fields even have the beneficial effect of reducing the intrinsic spatial resolution of the device, which is a consequence of the angular and energy distribution of the photoelectrons at emission from the photocathode [47]. HPDs have been incorporated as major components of a novel axial PET camera design discussed in section 5. Similarly, detectors based on hybrid photodetectors and configurations using wavelength shifting fibers have also been developed [48]. Notwithstanding, the use of semiconductor detectors in PET is far from reaching acceptance; these devices are regarded as especially promising candidates for the design of PET cameras with the aim of overcoming the drawbacks of conventional PMT-based PET instrumentation [43].

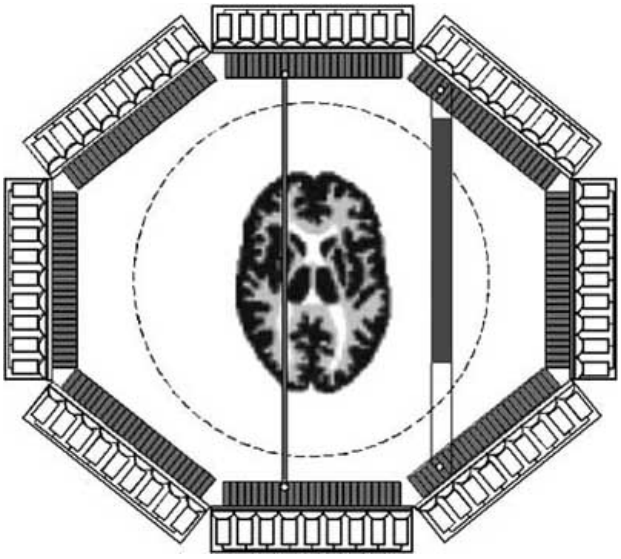

Fig. (3). Diagram showing the parallax or depth-of-interaction error associated with annihilations occurring off-centre of the transaxial field-of-view or oblique LoRs for a multi-ring PET scanner. Note the significant degradation of spatial resolution for off-centred LoRs.

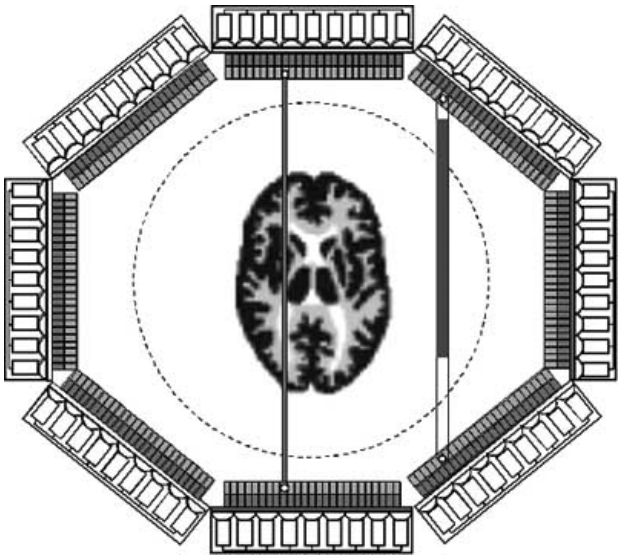

Fig. (4). Diagram showing the reduction of parallax or depth-of-interaction error when using the phoswich detector approach with depth-of-interaction measurement capability. The two detectors are assembled in a sandwich-like design and the difference in decay time of the light is used to estimate depth in the crystal where the interaction occurred. Note the reduction in degradation of spatial resolution for off-centred LoRs.

3. MOTIVATIONS FOR THE DEVELOPMENT OF DEDICATED BRAIN PET CAMERAS

In PET systems designed for human brain imaging, the ultimate performance in terms of spatial resolution, sensitivity and SNR, can be achieved through careful selection of the design geometry, detector assembly and readout electronics as well as optimized data acquisition protocols and image reconstruction algorithms. The rationale in designing dedicated brain *vs* multipurpose whole-body PET scanners resides in the fact that unlike whole-body imaging, where a larger detector ring diameter is needed to accommodate large patients, the size of the human head is relatively small, thus allowing to reduce the scanner's ring diameter and to increase the solid-angle coverage, leading to higher sensitivity per unit detector volume [17]. A small ring design has the advantage of improving the inherent spatial resolution degradation due to noncollinearity of the annihilation photons in addition to reducing the overall cost of the PET tomograph at the expense of a higher parallax error, hence an image degradation depending on the emission point in the transaxial plane and/or the angle of incidence of the lines of responses. This effect becomes worse when reducing the scanner's ring diameter or the size of the crystal's cross-sectional area. This inherent limitation could be coped with by keeping the radial length of the crystal small, typically on values around the attenuation length at 511 keV, which however strongly compromises the detection efficiency. As mentioned earlier, the phoswich approach, which leads to a better approximation of the interaction point, has recently been implemented in several designs and particularly in the HRRT [37]. Such an approach halves the parallax error for a given crystal length, but still only represents a compromise between maximum sensitivity and optimum spatial resolution.

In principle, a dedicated brain PET scanner should be able to provide higher spatial resolution, while at the same time offering a sufficiently high counting rate capability to allow investigation of physiological processes with fast temporal dynamics [49]. It is worth noting that 3-D data collection is now well accepted by the PET imaging community for brain imaging, in contrary to whole-body imaging where it is still subject to debate [50]. In this context, the noise equivalent counts (NEC) rate concept, which quantifies the useful counts being acquired after applying perfect correction techniques for the physical effects, has been extensively used to assess the real improvement obtained from 3-D *vs*. 2-D data collection strategies. The NEC does not, however, take into account all design or operational parameters that affect image quality. It has been shown that the peak NEC is obtained at a lower activity concentration in 3-D than in 2-D [51]. As a result, the SNR will be higher in the low activity concentration range when operating in 3-D mode than in 2-D. Moreover, 3-D brain imaging results in improved NEC rates for all activity levels, whereas for other body regions, relative 3-D/2-D gain will depend on activity level. This has important implications in clinical studies where reduction of the injected activities and hence the radiation dose to the patient is of concern [52].

4. STATE OF THE ART BRAIN PET INSTRUMENTATION

There has been a remarkable progress in PET instrumentation design from a single ring of BGO crystals with a spatial resolution of ~15 mm, to multiple rings of BGO and more recently, GSO and LSO detector blocks resulting in a spatial resolution of about 4-6 mm.

Improvements in spatial resolution have been achieved by the use of smaller crystals and the efficient use of light sharing schemes to identify the active detector cell. On the other hand, improvements in sensitivity have been accomplished through fully 3-D acquisition mode by removing the interplane septa, which increases coincidence efficiency by about a factor of around five in comparison to 2-D acquisition with interplane septa extended [19]. Newer tomographs operate essentially in fully 3-D acquisition geometries, at the expense of increasing system sensitivity to scattered radiation and random coincidences.

Several innovative developments in PET instrumentation have been proposed or are currently under design or test. These include large or pixelated detectors mounted on a rotating gantry, detectors arranged in a cylindrical partial or full multiring geometry, and detectors assembled in a polygonal ring. A high resolution PET camera design was proposed in the 90s by optimizing the detector size and system diameter through optimal arrangement of a small number of large detectors in a circular ring format combined with a dedicated sampling scheme [53]. Monte Carlo simulation studies showed that the proposed design allows to obtain uniform high-resolution (2-3 mm FWHM) images [54]. Another interesting contribution highlighted the advantages of designing a spherical PET geometry, taking advantage of the large solid angle of acceptance, which results in improved system sensitivity and image SNR [55]. A conceptual design of a PET camera dedicated for isotropic high resolution human brain and small animal imaging was presented by Moses *et al*. [56]. The LSO-based detector modules are capable of DOI measurement, which is incorporated into the reconstruction algorithm by rebinning onto a regularly spaced grid. Monte Carlo simulation results demonstrated that with a DOI measurement resolution of 5 mm FWHM, the spatial resolution becomes essentially uniform (2.5-3.0 mm FWHM) throughout the field-of-view (FOV) and insensitive to ring diameter (between 30 and 40 cm). Likewise, the HEAD PENN-PET scanner design is based on the use of six hexagonally arranged flat NaI(TI) detectors, which allows a unique arrangement of single annular crystals in a cost-effective design [57]. This design offers a large axial acceptance angle and high sampling density along all three axes without scanner motion and was successfully used for clinical brain studies and pediatric whole-body oncological studies.

In order to meet the objectives set by the biomedical imaging research community, new generation high-resolution 3D-only brain PET tomographs have been designed. Current existing commercial brain PET technology (e.g. the ECAT-HRRT developed by CPS-Innovations [37]) and recent dedicated prototype designs including G-PET [49] and Hamamatsu SHR-12000 [58] constitute state of the art high-resolution PET instrumentation dedicated for brain research. Fig. **5** illustrates photographs of the above-mentioned designs adopted by scanner manufacturers and research groups. The HRRT consists of octagonal arrangements (42.4 cm face-to-face) of phoswich scintillator block detectors made of two layers of 64 small LSO crystals

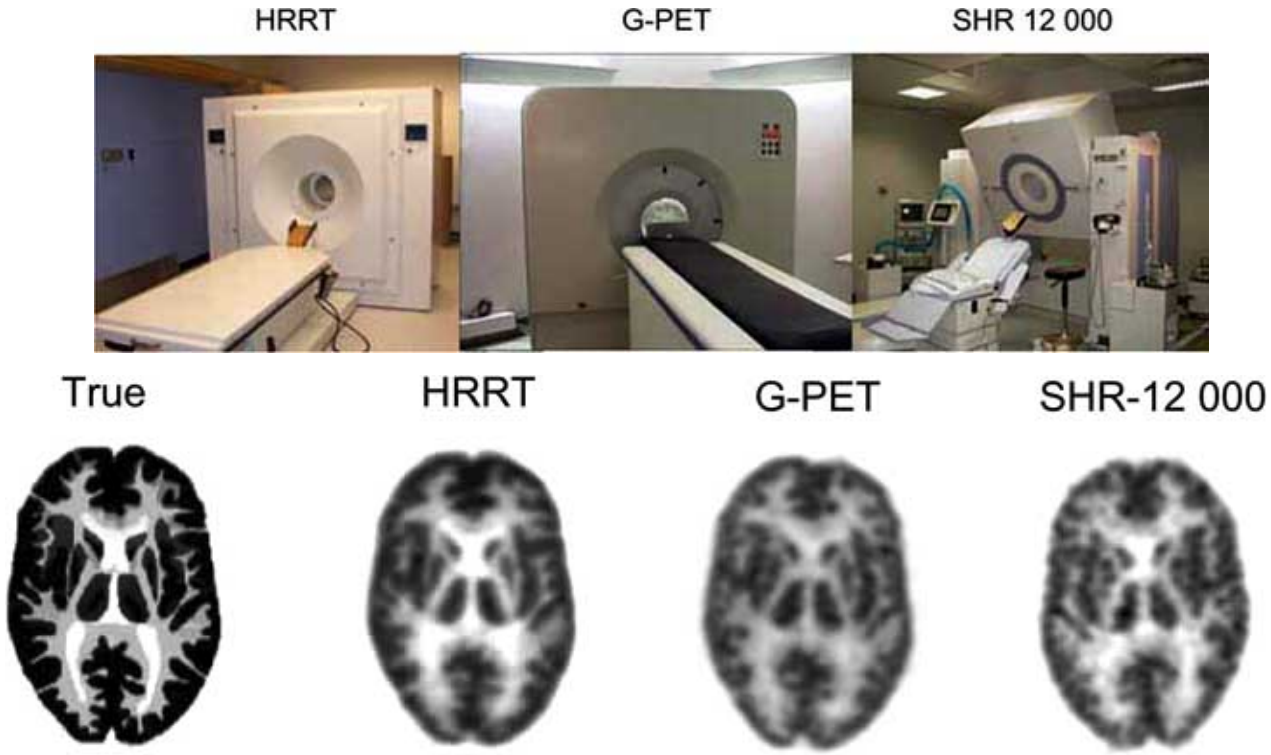

Fig. (5). Photographs of dedicated brain PET scanners showing from left to right the HRRT camera using LSO scintillation crystals and the phoswich concept, the GSO-based PET (G-PET) camera, and the Hamamatsu SHR-12 000 PET scanner based on BGO detector blocks. **B.** Representative images of the Hoffman 3-D brain phantom acquired on the above mentioned PET scanners are shown. It should be emphasized that the data collection and reconstruction procedures were not similar (Photographs and images courtesy of Dr Watanabe, Dr Surti, Dr Sossi and Prof. Wienhard).

(each 2.1 x 2.1 x 7.5 mm^3) with 2 different decay times ($\Delta\tau$~7 ns). The crystals (15 mm total active length) are oriented normal to the octagon sides, hence, essentially pointing in radial direction. The geometry of the G-PET brain scanner developed at the University of Pennsylvania is similar to the HEAD PENN-PET mentioned above; however, the detector technology and electronic components have been improved to achieve improved performance. This scanner has a detector ring diameter of 42.0 cm and an axial FOV of 25.6 cm and operates only in fully 3-D mode. It comprises a total of 18,560 (320 x 58 array) 4 x 4 x 10 mm^3 GSO crystals coupled through a continuous light-guide to 288 (36 x 8 array) 39 mm PMT's in a hexagonal arrangement. On the other hand, the gantry and bed motions of the Hamamatsu SHR-12000 were designed specifically to allow subjects' scanning in lying, sitting and standing postures, thus giving the possibility to research investigators to perform activation studies with high flexibility. This scanner has a diameter of 50.8 cm and an axial FOV of 16.3 cm. It comprises a total of 11,520 crystals arranged in 24 detector rings and 8x4 (2.8 x 6.55 x 30 mm^3 per crystal) BGO detector blocks readout by compact PS-PMT's. The scanner can be operated in 2-D or 3-D data acquisition modes when the interplane septa are retracted but the evaluation in 3-D mode has not been completed yet.

None of the above PET systems has the ideal physical characteristics required to make it the gold standard reference for clinical and research applications. Each design has its own advantages and drawbacks, and it is up to the user or research investigator to select the most appropriate camera for the considered range of applications. It is worth emphasizing that, given the low demand, most dedicated PET tomographs described in this paper consist of prototypes developed by research groups. The HRRT is the only prototype commercially available, which could hopefully be designed according to the desires of the user. As an example, a version of this camera based on a single LSO crystal layer (HRRT-S) of 7.5 mm thickness has been delivered to Amsterdam PET Centre [59].

4. NEW FRONTIERS IN BRAIN PET IMAGING TECHNOLOGY

4.1. Innovations in Brain PET Instrumentation

The demand for functional, metabolic, and molecular imaging of the brain has stimulated the development of dedicated high-resolution PET systems [60]. As in whole-body imaging, both high detection sensitivity and excellent spatial resolution are priorities for imaging system design and are needed to achieve suitable levels of image quality and quantitative accuracy. Thus, different PET designs have been or are being developed in both academic and corporate settings, with many such devices being offered commercially. More recently, advanced versions of these technologies have begun to be used in the study of brain function in a myriad of experimental settings.

Considering the existing instrumentation and components, the intrinsic physical performance of conventional PET designs, which rely on the classical radial arrangement of scintillation crystals, is approaching the fundamental limits. This has encouraged the development of innovative approaches capable of providing improved performance at a reduced or comparable cost to current technologies. The goal is to maximize the detection efficiency for annihilation photons and, at the same time, to push the spatial resolution towards the physical limits inherent to the annihilation process as determined by the positron range in organic tissues and the noncollinearity of the annihilation photons. For example, Braem *et al*. [40] have proposed a novel detector design, which provides full 3-D reconstruction free of parallax errors with excellent spatial resolution over the total detector volume. The key components are a matrix of long scintillator crystals coupled on both ends to HPDs with matched segmentation and integrated readout electronics. The data acquisition system is composed of several read out cards (each one associated with a module of the PET scanner) and a main card that controls the whole system [61]. Using fast triggering signals from the silicon sensor back-planes, the main card performs the coincidence event analysis and enables the read out of the two modules involved in case of coincidence. The other modules are left free to perform new acquisitions. This concept based on several independent, event driven and parallel read out chains, considerably reduces the acquisition dead time. Computer simulations and Monte Carlo modeling predict that the detector will achieve excellent spatial (x,y,z) and energy resolution [62]. The design also increases detection efficiency by reconstructing a significant fraction of events that undergo Compton scattering in the crystals. The 3-D axial detector geometry (Fig. **6**) is configured from a matrix of 208 (13x16) long crystals, each with a cross section of 3.2x3.2 mm^2 and with an intercrystal spacing of

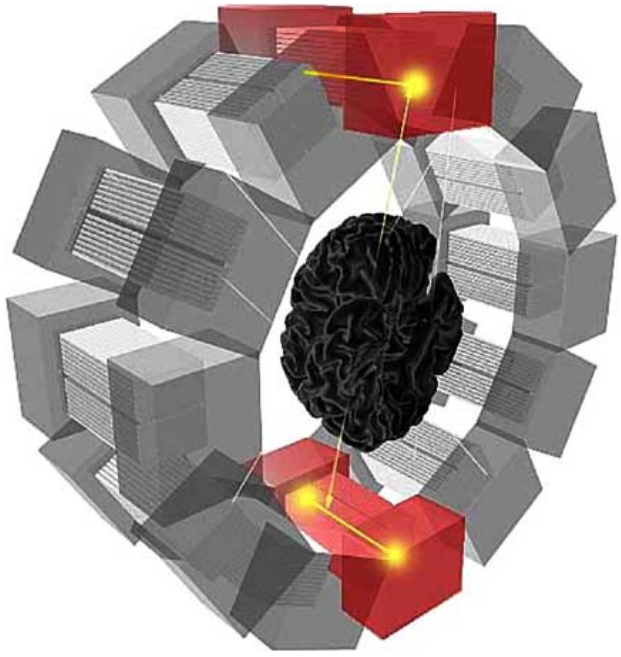

Fig. (6). Illustration of principles of data acquisition for the proposed axial 3-D brain PET camera using the novel design based on 12 camera modules consisting of long scintillation crystals readout on both sides by HPDs. Reprinted with permission from Braem *et al*. [40].

0.8 mm. Scintillation light produced after an interaction of an annihilation photon will propagate by total internal reflection to the ends of the crystal, where it will be detected by the HPD photodetectors. The transaxial resolution depends only on the crystal segmentation and not on its chemical composition, whereas the axial resolution is closely related to the scintillator properties. The scintillator's optical bulk absorption length should be approximately equal to the crystal length to obtain both a high light yield and a signify-cant light asymmetry required to decode the axial coordinate *z* of the photon interaction in the crystal matrix [63].

Likewise, many conceptual designs developed specifically for small animal and non-human primates imaging could be applied equally well to high resolution human brain imaging by increasing detector ring diameter and adapting the detector components accordingly. One such example is the clearPET Neuro scanner dedicated for non-human primates imaging [64], which uses a phoswich detector block combining two 10 mm crystal layers of lutetium-based (LSO:Ce and LuYAP:Ce) scintillators (see Table **1**) segmented into 64 (8x8) detection elements, with a cross section of 2x2 mm^2 coupled to multi-channel photomultiplier tubes. The opening diameter of the ring is variable between 13 and 30 cm for an axial field-of-view of 11 cm, whereas the transaxial field-of-view is adjustable per software. Likewise, the recent growth of scintillation crystals having very high light output and stopping power, excellent energy resolution and fast timing properties spurred the development of time-of-flight PET-based iterative reconstruction strategies, which proved to provide much faster convergence compared to conventional reconstruction consistently improving the SNR ratio [65].

4.2. Developments in Multimodality Imaging

During the course of patient diagnosis, anatomical imaging is usually performed with techniques such as CT or MRI that have excellent spatial resolution and SNR characteristics, but that may offer relatively low specificity for differentiating disease from normal structures. In opposition, PET generally targets a specific functional or metabolic signature in a way that can be highly specific, but generally lacks spatial resolution and anatomical evidence which often are needed to localize or stage the disease, or for planning therapy in cancers of the brain, head and neck. The availability of correlated functional and anatomical images improves the detection of disease by highlighting areas of increased radiotracer uptake on the anatomical CT or MRI scan, whereas regions that look abnormal in the anatomical image can draw attention to a potential area of disease where radiopharmaceutical uptake may be low [29]. There have been multiple studies which have demonstrated the role of PET/CT especially for improved characterization of equivocal lesions in oncologic applications, thus impacting patients' management [66]. Likewise, fused PET/MRI data was used extensively in a wide variety of clinical neurological applications including cerebrovascular disorders, brain trauma, stroke, epilepsy, dementia, Parkinson's disease and brain tumors, and in mental disorders such as depression, schizophrenia and obsessive-compulsive disorders as well as localization of functional neuroactivation detected with PET.

Much research and development has also concentrated on the development of multi-modality image registration algorithms required to improve the correlation between anatomical (CT and MRI) and physiological information involving PET or SPECT both in clinical and research settings. Software-based image registration allows to fuse images from two or more different modalities after they are acquired separately [28]. The simplest form of image co-registration uses "rigid-body" translation and rotation to match the two image data sets. These techniques can be applied most successfully to neurological studies, where the skull provides a rigid structure that maintains the geometrical relationship of structures within the brain and are now used routinely for clinical procedures at most institutions [67, 68]. Figure **7** illustrates an example of fusion of clinical brain MRI with ^{18}F-FDG PET after image co-registration. In more

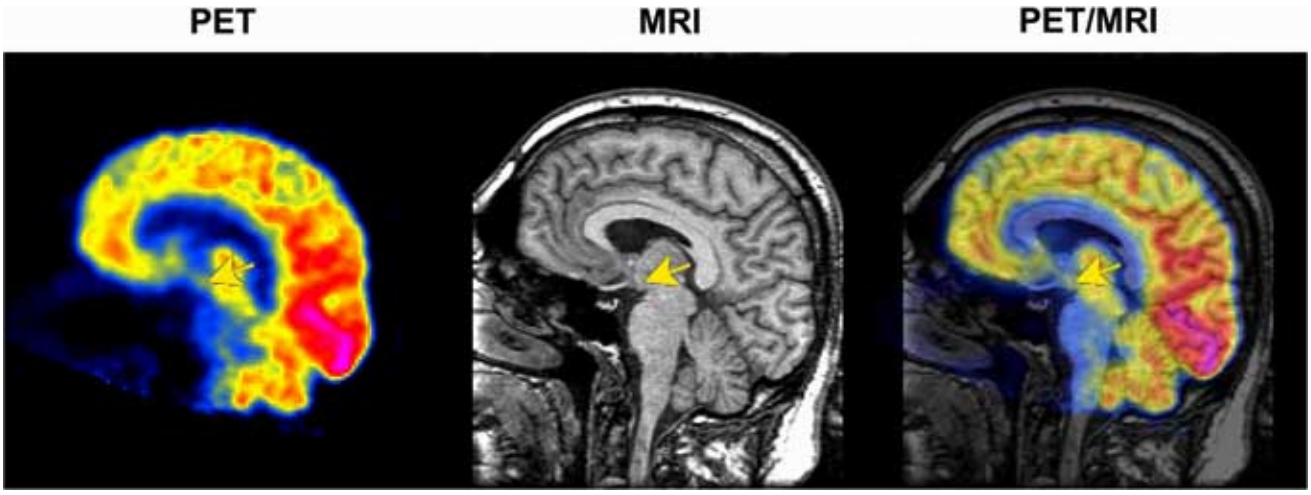

Fig. (7). Example of image fusion of morphological MRI with functional ^{18}F-FDG PET images of a clinical brain study. The high resolution MRI may allow the identification of the anatomic boundaries of different cerebral structures to define precisely the regions of interest for the purposes of quantification or for partial volume correction. From left to right: MRI, PET, and the fused MRI/PET image.

basic research studies, the co-registration of brain PET with MRI could be used for automatic delineation of 3-D volumes of interest (VOI's) on an MRI dataset to quantify radionuclide uptake in a co-registered PET study [69] or alternatively for attenuation compensation [70] and partial volume correction [71, 72] of PET data, thus enhancing its quantitative accuracy. Although such methods are fully automated, their performance depends on many physiological and technical aspects; further research is being conducted to evaluate their suitability in different clinical situations and their potential use in motion correction frequently encountered during lengthy PET scanning protocols.

While all clinical and commercial dual-modality systems have been configured in the form of PET/CT or SPECT/CT scanners, several investigators proposed and in some cases, have implemented and tested prototype dual-modality systems that combine MRI with PET [73-78]. There are, however, several important challenges that must be overcome in implementing and operating a combined PET/MRI imaging system. In comparison to x-ray CT, MRI typically is more expensive, involves longer scan times, and produces anatomical images from which it is more difficult to derive attenuation maps for attenuation correction of the PET data [70]. Furthermore, virtually all clinical PET imaging systems use PMT's as photodetectors whose performance can be seriously affected in the presence of magnetic fields, which are significantly smaller than those produced by modern MRI scanners. This is especially problematic in an MRI scanner which relies on rapidly switching gradient magnetic fields and radiofrequency (RF) signals to produce the magnetic resonance image. The presence of the magnetic field gradients and RF signals certainly could disrupt the performance of a PMT and PET detector if they were located within or adjacent to the magnet of the MRI system. Similarly, the operation of the MRI system relies on a very uniform and stable magnetic field to produce the MR image. The introduction of radiation detectors, electronics, and other bulk materials can perturb the magnetic field in a way that introduces artifacts in the MR image.

4.3. Developments in Quantification

By its very nature, PET is a quantitative imaging process. However, quantitative PET imaging requires a variety of skills, resources and personnel, beyond what is needed for routine clinical imaging. Facilities specializing in PET-based functional neuroimaging research are usually populated by multi-disciplinary groups of scientists. The common goal of these investigators is to develop, test, and validate tools for producing quantitative regional estimates of physiological parameters from dynamic radiotracer studies. Fig. **8** visualizes image quality degradation by comparing an ideal ^{18}F-FDG PET study of the Hoffman 3-D brain phantom without any physical or instrumentation-based limitation and a realistic brain PET study obtained by Monte Carlo simulations including all degradation effects. The differences in image quality between both images mainly consist of degraded spatial resolution and contrast resolution, due to limited system resolution, contribution from scattered events, and the limitations of the reconstruction algorithm. The difference is striking and shows how complicated it will be to properly obtain a correct activity quantification from PET imaging.

Much worthwhile effort has been spent on the development of accurate models for high resolution Bayesian reconstruction and improved quantification of molecular targets using combined PET/MR imaging through the implementation of sophisticated algorithms to compensate for physical degrading factors (e.g. attenuation, scatter, partial volume effect). However, none of the methods published so far was user-independent and accurate enough for wide acceptance by the medical imaging community [79]. Moreover, evaluation and clinical validation of image reconstruction algorithms are inherently difficult and sometimes unconvincing. Examples of patient studies displaying brain PET images are generally used as indicators of image quality, but, because truth in these studies is seldom known, experimentally measured or simulated data are often used for a more objective analysis. There is a clear need for guidelines to evaluate reconstruction techniques and other image processing issues in PET. Further research and

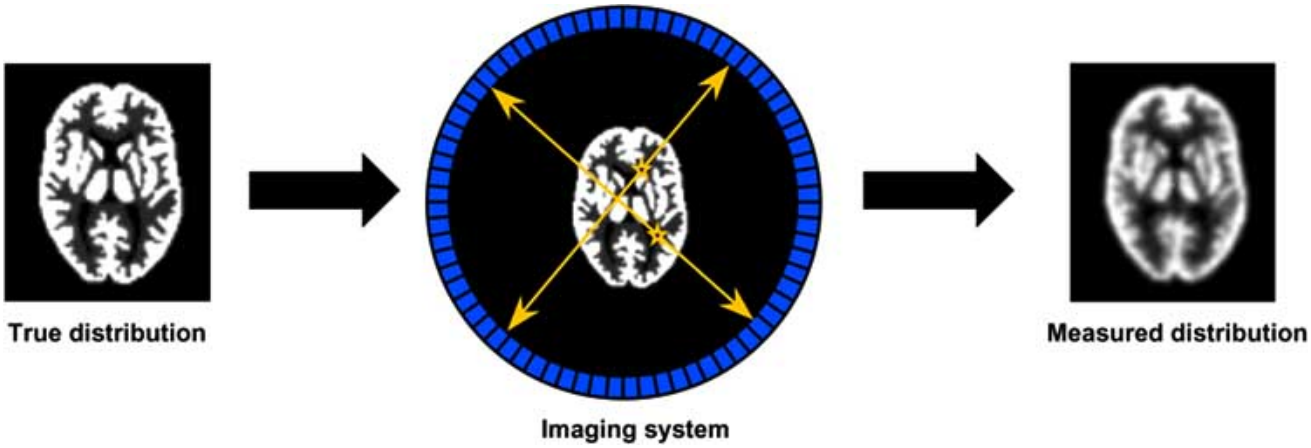

Fig. (8). Principle of PET data acquisition showing expected differences in terms of image quality between the true activity distribution (left) and measured activity distribution (right) in the Hoffman 3-D brain phantom. The differences are mainly due to intrinsic limitations of the PET scanner and inherent imperfections of image correction and reconstruction techniques.

development efforts are therefore still required to come up with a unified framework for optimal data collection, reconstruction and quantification in 3-D brain PET.

5. CONCLUSION AND FUTURE PERSPECTIVES

Despite major advances in imaging instrumentation, PET technology dedicated for neuroimaging is still limited by low spatial resolution, sensitivity and count rate performance, in addition to being clinically under-utilized. The capabilities of brain PET instrumentation have undergone continual, and sometimes abrupt improvements in performance and in their sophistication and complexity. A baseline of performance can be assessed by physicists who use objective measures of spatial resolution, energy resolution, count-rate response, and other parameters to assess the technical capabilities of commercial and research systems. New developments in PET instrumentation are taking advantage of recent progress made in high energy physics experiments in connection with the development of new detector materials like inorganic scintillators of high density, atomic number and light yield as well as photodetectors. A similar trend has come up through advances in microelectronic technologies, which have led to highly integrated CMOS front-end circuits, fast data acquisition processors and ultra rapid field programmable gate arrays (FPGAs). Several high-resolution PET scanner designs dedicated for brain imaging have been or are being developed in both academic and corporate settings, with some devices being offered commercially, leading the nuclear medicine community to forecast a promising progress during the next few years. Thus, many different design paths have been and continue to be pursued in both academic and corporate settings, that offer different trade-offs in terms of their performance. It is still uncertain which designs will be incorporated into future clinical and research systems, but it is certain that technological advances will continue and will enable new quantitative capabilities in brain PET imaging.

ACKNOWLEDGEMENTS

This work was supported in part by the Swiss National Science Foundation under grant SNSF 3152A0-102143 and the Research and Development Foundation of Geneva University Hospital under grant PRD-04-1-08.

REFERENCES

[1] Nutt R. The history of positron emission tomography. Mol Imaging Biol 2002; 4: 11-26.

[2] Wrenn FR. Jr, Good ML, Handler P. The use of positron-emitting radioisotopes for the localization of brain tumors. Science 1951; 113: 525-527.

[3] Sweet WH. The uses of nuclear disintegration in the diagnosis and treatment of brain tumor. N Engl J Med 1951; 245: 875-878.

[4] Brownell GL, Sweet WH. Localization of brain tumors with positron emitters. Nucleonics 1953; 11: 40-45.

[5] Phelps ME, Hoffman EJ, Mullani NA, Higgins CS, Ter-Pogossian MM. Design considerations for a positron emission transaxial tomograph (PETT III). IEEE Tran Nucl Sci 1976; NS-23: 516-522.

[6] Hoffman EJ, Phelps ME, Mullani N, Higgins CS, Sobel BE, Ter-Pogossian MM. Design and performance characteristics of a whole-body transaxial tomograph. J Nucl Med 1976; 17: 493–502.

[7] Jones T, Chesler DA, Ter-Pogossian MM. The continuous inhalation of oxygen-15 for assessing regional oxygen extraction in the brain of man. Br J Radiol 1976; 49: 339-343.

[8] Thompson CJ, Yamamoto YL, Meyer E. Positome II: A high efficiency positron imaging device for dynamic brain studies. IEEE Trans Nucl Sci 1979; 26: 583-589.

[9] Ter-Pogossian MM, Mullani NA, Hood JT, Higgins CS, Ficke DC. Design considerations for a positron emission transverse tomograph (PETT V) for imaging of the brain. J Comput Assist Tomogr 1978; 2: 539-544.

[10] Ter-Pogossian MM, Ficke DC, Hood JT Sr., Yamamoto M, Mullani NA. PETT VI: a positron emission tomograph utilizing cesium fluoride scintillation detectors. J Comput Assist Tomogr 1982; 6: 125-133.

[11] Nohara N, Tanaka E, Tomitani T, *et al*. Positologica: A positron ECT device with a continuously rotating detector ring. IEEE Trans Nucl Sci 1980; 27: 1128-1136.

[12] Kanno I, Uemura K, Miura S, Miura Y. HEADTOME: a hybrid emission tomograph for single photon and positron emission imaging of the brain. J Comput Assist Tomogr 1981; 5: 216-226.

[13] Brooks RA, Sank VJ, Di Chiro G, Friauf WS, Leighton SB. Design of a high resolution positron emission tomograph: the Neuro-PET. J Comput Assist Tomogr 1980; 4: 5-13.

[14] Litton J, Bergstrom M, Eriksson L, Bohm C, Blomqvist G, Kesselberg M. Performance study of the PC-384 positron camera system for emission tomography of the brain. J Comput Assist Tomogr 1984; 8: 74-87.

[15] Holte S, Eriksson L, Dahlbom M. A preliminary evaluation of the Scanditronix PC2048-15B brain scanner. Eur J Nucl Med 1989; 15: 719-721.

[16] Williams CW, Crabtree MC, Burke MR, *et al*. Design of the NeuroECAT: A high-resolution, high-efficiency positron tomograph for imaging the adul head or infant torso. IEEE Tran Nucl Sci 1981; 28: 1736-1740.

[17] Hoffman EJ, Phelps ME, Huang SC. Performance evaluation of a positron tomograph designed for brain imaging. J Nucl Med 1983; 24: 245-257.

[18] Yamashita T, Uchida H, Okada H, *et al*. Development of a high resolution PET. IEEE Trans Nucl Sci 1990; 37: 594-599.

[19] Spinks TJ, Jones T, Bailey DL, *et al*. Physical performance of a positron tomograph for brain imaging with retractable septa. Phys Med Biol 1992; 37: 1637-1655.

[20] Mullani NA, Gould KL, Hartz RK, *et al.* Design and performance of POSICAM 6.5 BGO positron camera. J Nucl Med 1990; 31: 610-616.

[21] DeGrado TR, Turkington TG, Williams JJ, Stearns CW, Hoffman JM, Coleman RE. Performance characteristics of a whole-body PET scanner. J Nucl Med 1994; 35: 1398-1406.

[22] Wienhard K, Dahlbom M, Eriksson L, *et al*. The ECAT EXACT HR: performance of a new high resolution positron scanner. J Comput Assist Tomogr 1994; 18: 110-118.

[23] Adam LE, Karp JS, Daube-Witherspoon ME, Smith RJ. Performance of a whole-body PET scanner using curve-plate NaI(Tl) detectors. J Nucl Med 2001; 42: 1821-1830.

[24] Surti S, Karp JS. Imaging characteristics of a 3-dimensional GSO whole-body PET camera. J Nucl Med 2004; 45: 1040-1049.

[25] Bettinardi V, Danna M, Savi A, *et al.* Performance evaluation of the new whole-body PET/CT scanner: Discovery ST. Eur J Nucl Med Mol Imaging 2004; 31: 867-881.

[26] Erdi YE, Nehmeh SA, Mulnix T, Humm JL, Watson CC. PET performance measurements for an LSO-based combined PET/CT scanner using the National Electrical Manufacturers Association NU 2-2001 standard. J Nucl Med 2004; 45: 813-821.

[27] Phelps ME, Cherry SR. The changing design of positron imaging systems. Clin Pos Imag 1998; 1: 31-45.

[28] Hutton BF, Braun M. Software for image registration: algorithms, accuracy, efficacy. Semin Nucl Med 2003; 33: 180-192.

[29] Hasegawa B, Zaidi H. "Dual-modality imaging: more than the sum of its components" In Ed. H. Zaidi. Quantitative analysis in nuclear medicine imaging. New York, Springer. 2005; 35-81.

[30] Townsend DW, Cherry SR. Combining anatomy and function: the path to true image fusion. Eur Radiol 2001; 11: 1968-1974.

[31] Marsden PK. Detector technology challenges for nuclear medicine and PET Nucl Instr Methods A 2003; 513: 1-7.

[32] Derenzo SE, Weber MJ, Bourret-Courchesne E, Klintenberg MK. The quest for the ideal inorganic scintillator. Nucl Instr Meth A 2003; 505: 111-117.

[33] van Eijk CWE. Inorganic scintillators in medical imaging. Phys Med Biol 2002; 47: R85-R106.

[34] Ter-Pogossian MM, Mullani NA, Ficke DC, Markham J, Snyder DL. Photon time-of-flight-assisted positron emission tomography. J Comput Assist Tomogr 1981; 5: 227-239.

[35] Surti S, Karp JS, Muehllehner G. Image quality assessment of LaBr3-based whole-body 3D PET scanners: a Monte Carlo evaluation. Phys Med Biol 2004; 49: 4593-4610.

[36] Dorenbos P. Light output and energy resolution of Ce3+-doped scintillators. Nucl Instr Meth A 2002; 486: 208-213.

[37] Wienhard K, Schmand M, Casey ME, *et al.* The ECAT HRRT: performance and first clinical application of the new high resolution research tomograph. IEEE Trans Nucl Sci 2002; 49: 104 -110.

[38] Casey ME, Nutt RA. A multicrystal two dimensional BGO detector system for Positron Emission Tomography. IEEE Trans Nucl Sci 1986; NS 33: 460-463.

[39] Dahlbom M, MacDonald LR, Schmand M, Eriksson L, Andreaco M, Williams C. A YSO/LSO phoswich array detector for single and coincidence photon imaging. IEEE Trans Nucl Sci 1998; 45: 1128-1132.

[40] Braem A, Chamizo Llatas M, Chesi E, *et al*. Feasibility of a novel design of high-resolution parallax-free Compton enhanced PET scanner dedicated to brain research. Phys Med Biol 2004; 49: 2547-2562.

[41] Shimizu K, Ohmura T, Watanabe M, Uchida H, Yamashita T. Development of 3-D detector system for positron CT. IEEE Trans Nucl Sci 1988; 35: 717-720.

[42] Del Guerra A, Bisogni MG, Damiani C, Di Domenico G, Marchesini R, Zavattini G. New developments in photodetection for medicine. Nucl Instr Methods A 2000; 442: 18-25.

[43] Humm JL, Rosenfeld A, Del Guerra A. From PET detectors to PET scanners. Eur J Nucl Med Mol Imaging 2003; 30: 1574-1597.

[44] Renker D. Properties of avalanche photodiodes for applications in high energy physics, astrophysics and medical imaging. Nucl Instr Meth A 2002; 486: 164-169.

[45] Joram C. Large area hybrid photodiodes. Nucl Phys B 1999; 78: 407-415.

[46] Weilhammer P. Silicon-based HPD development: sensors and front ends. Nucl Instr Meth A 2000; 446: 289-298.

[47] D'Ambrosio C, Leutz H. Hybrid photon detectors. Nucl Instr Meth A 2003; 501: 463-498.

[48] Worstell W, Johnson O, Kudrolli H, Zavarzin V. First results with high-resolution PET detector modules using wavelength-shifting fibers. IEEE Trans Nucl Sci 1998; 45: 2993-2999.

[49] Karp JS, Surti S, Daube_Witherspoon ME, *et al.* Performance of a brain PET camera based on anger-logic gadolinium oxyorthosilicate detectors. J Nucl Med 2003; 44: 1340-1349.

[50] Lartizien C, Kinahan PE, Comtat C. A lesion detection observer study comparing 2-dimensional versus fully 3-dimensional whole-body PET imaging protocols. J Nucl Med 2004; 45: 714-723.

[51] Bendriem B, Townsend DW. "The theory and practice of 3D PET,". Dordrecht: Kluwer Academic Publishers, The Netherlands, 1998.

[52] Lartizien C, Comtat C, Kinahan PE, Ferreira N, Bendriem B, Trebossen R. Optimization of injected dose based on noise equivalent count rates for 2- and 3-dimensional whole-body PET. J Nucl Med 2002; 43: 1268-1278.

[53] Cho ZH, Juh SC, Friedenberg RM, Bunney W, Buchsbaum M, Wong E. A new approach to very high resolution mini-brain PET using a small number of large detectors. IEEE Trans Nucl Sci 1990; 37: 842-851.

[54] Cho ZH, Juh SC. High resolution brain PET with large detectors. II Performance study. IEEE Trans Nucl Sci 1991; 38: 726-731.

[55] Ficke D, Hood J, Ter-Pogossian M. A spheroid positron emission tomograph for brain imaging: a feasibility study. J Nucl Med 1996; 37: 1219-1225.

[56] Moses WW, Virador PRG, Derenzo SE, Huesman RH, Budinger TF. Design of a high-resolution, high-sensitivity PET camera for human brains and small animals. IEEE Trans Nucl Sci 1997; 44: 1487-1491.

[57] Karp JS, Freifelder R, Geagan MJ, *et al.* Three-dimensional imaging characteristics of the HEAD PENN-PET scanner. J Nucl Med 1997; 38: 636-643.

[58] Watanabe M, Shimizu K, Omura T, *et al*. A new high-resolution PET scanner dedicated to brain research. IEEE Trans Nucl Sci 2002; 49: 634-639.

[59] Boellaard R, Buijs F, de Jong HWAM, Lenox M, Gremillion T, Lammertsma AA. Characterization of a single LSO crystal layer High Resolution Research Tomograph. Phys Med Biol 2003; 48: 429-448.

[60] Sossi V. Positron emission tomography (PET) advances in neurological applications. Nucl Instr Methods A 2003; 510: 107-115.

[61] Dragone A, Corsi F, Marzocca C, *et al*. An event driven read-out system for a novel PET scanner with Compton-enhanced 3D gamma reconstruction. IEEE Trans Nucl Sci 2005; 52: *in press*

[62] Seguinot J, Braem A, Chesi E, *et al.* Novel geometrical concept of high performance brain PET scanner: Principle, design and performance estimates. Nucl Instr Meth A 2005; *submitted*

[63] Braem A, Chamizo Llatas M, Chesi E, *et al.* Novel design of a parallax free Compton enhanced PET scanner. Nucl Instr Methods A 2004; 525: 268-274.

[64] Ziemons K, Achten R, Bauer A, *et al.* "The ClearPET neuro scanner: A LSO/LuYAP phoswich small animal PET scanner" IEEE Nuclear Science Symposium and Medical Imaging Conference, Oct. 19-22, Rome, Italy, 2004.

[65] Conti M, Casey ME, Kehren F. "Implementation of time-of-flight on CPS HiRez PET scanner" IEEE Nuclear Science Symposium and Medical Imaging Conference, Oct. 19-22, Rome, Italy, 2004.

[66] Cohade C, Wahl RL. Applications of positron emission tomography/computed tomography image fusion in clinical positron emission tomography - clinical use, interpretation, methods, diagnostic improvements. Semin Nucl Med 2003; 33: 228-237.

[67] Pietrzyk U, Herholz K, Fink G, *et al.* An interactive technique for three-dimensional image registration: validation for PET, SPECT, MRI and CT brain studies. J Nucl Med 1994; 35: 2011-2018.

[68] Woods RP, Grafton ST, Holmes CJ, Cherry SR, Mazziotta JC. Automated image registration: I. General methods and intrasubject, intramodality validation. J Comput Assist Tomogr 1998; 22: 139-152.

[69] Svarer C, Madsen K, Hasselbalch SG, *et al.* MR-based automatic delineation of volumes of interest in human brain PET images using probability maps. Neuroimage 2005; 24: 969-979.

[70] Zaidi H, Montandon M-L, Slosman DO. Magnetic resonance imaging-guided attenuation and scatter corrections in three-dimensional brain positron emission tomography. Med Phys 2003; 30: 937-948.

[71] Rousset OG, Ma Y, Evans AC. Correction for partial volume effects in PET: principle and validation. J Nucl Med 1998; 39: 904-911.

[72] Baete K, Nuyts J, Van Laere K, *et al*. Evaluation of anatomy based reconstruction for partial volume correction in brain FDG-PET. Neuroimage 2004; 23: 305-317.

[73] Christensen NL, Hammer BE, Heil BG, Fetterly K. Positron emission tomography within a magnetic field using photomultiplier tubes and light-guides. Phys Med Biol 1995; 40: 691-697.

[74] Shao Y, Cherry SR, Farahani K, Meadors K. Simultaneous PET and MR imaging. Phys Med Biol 1997; 42: 1965-1970.

[75] Shao Y, Cherry SR, Farahani K, Slates R. Development of a PET detector system compatible with MRI/NMR systems. IEEE Trans Nucl Sci 1997; 44: 1167-1171.

[76] Slates R, Cherry SR, Boutefnouchet A, Shao Y, Dalhbom M, Farahani K. Design of a small animal MR compatible PET scanner. IEEE Trans Nucl Sci 1999; 46: 565-570.

[77] Slates R, Farahani K, Shao Y, *et al.* A study of artefacts in simultaneous PET and MR imaging using a prototype MR comptatible PET scanner. Phys Med Biol 1999; 44: 2015-2027.

[78] Yamamoto S, Takamatsu S, Murayama H, Minato K. A block detector for a multislice, depth-of-interaction MR-compatible PET. EEE Trans Nucl Sci 2005; 52: 33-37.

[79] Zaidi H, Sossi V. Correction for image degrading factors is essential for accurate quantification of brain function using PET. Med Phys 2004; 31: 423-426.

Received: February 14, 2005 Revised: June 03, 2005 Accepted: June 09, 2005